Hannes Radner, Lars Büttner, Jürgen Czarske

Interferometric velocity measurements through a fluctuating interface using a Fresnel guide star-based wavefront correction system

Erstveröffentlichung in / First published in:

Optical Engineering. 2018, 57(8), S. 084104-1 – 0084104-7 [Zugriff am: 23.05.2019]. SPIE Digital Library. ISSN 1560-2303.

DOI: https://doi.org/10.1117/1.OE.57.8.084104

Optical Engineering

OpticalEngineering.SPIEDigitalLibrary.org

Interferometric velocity measurements through a fluctuating interface using a Fresnel guide star-based wavefront correction system

Hannes Radner
Lars Büttner
Jürgen Czarske

SPIE.

Hannes Radner, Lars Büttner, Jürgen Czarske, "Interferometric velocity measurements through a fluctuating interface using a Fresnel guide star-based wavefront correction system," *Opt. Eng.* **57**(8), 084104 (2018), doi: 10.1117/1.OE.57.8.084104.

Interferometric velocity measurements through a fluctuating interface using a Fresnel guide star-based wavefront correction system

Hannes Radner,* Lars Büttner, and Jürgen Czarske
Technische Universität Dresden, Laboratory for Measurement and Sensor System Techniques, Faculty of Electrical and Computer Engineering, Dresden, Germany

Abstract. To improve optical measurements, which are degraded by optical distortions, wavefront correction systems can be used. Generally, these systems evaluate a guide star in transmission. The guide star emits well-known wavefronts, which sample the distortion by propagating through it. The system is able to directly measure the distortion and correct it. There are setups, where it is not possible to generate a guide star behind the distortion. Here, we consider a liquid jet with a radially open surface. A Mach–Zehnder interferometer is presented where both beams are stabilized through a fluctuating liquid jet surface with the Fresnel guide star (FGS) technique. The wavefront correction system estimates the beam path behind the surface by evaluating the incident beam angle and reflected beam angle of the Fresnel reflex with an observer to control the incident angle for the desired beam path. With this approach, only one optical access through the phase boundary is needed for the measurement, which can be traversed over a range of 250 μm with a significantly increased rate of valid signals. The experiment demonstrates the potential of the FGS technique for measurements through fluctuating phase boundaries, such as film flows or jets. [DOI: 10.1117/1.OE.57.8.084104]

Keywords: laser Doppler velocimetry; adaptive optics; wavefront compensation; Fresnel guide star.

Paper 180666 received May 7, 2018; accepted for publication Aug. 7, 2018; published online Aug. 25, 2018.

1 Introduction

Optical distortions are a common challenge for laser instrumentation as they can increase the measurement uncertainty or inhibit the measurement.

To compensate optical distortions, wavefront correction systems can be used.[1–10] They were first integrated in earth-bound telescopes to correct for the seeing effect, where fluctuating refractive index changes in the atmosphere distort the starlight.[10] These telescopes use a laser to generate fluorescence emission at high altitudes, acting as a guide star. This point source emits known spherical wavefronts that are distorted equally to the starlight. The distortion can be measured in transmission with a wavefront sensor inside the telescope to steer an adaptive mirror to correct the wavefront aberrations.

The guide star concept was soon adapted for optical metrology. For example, guide stars can also be generated by moving particles,[11] fluorescent particles,[12,13] second harmonic generation,[14] or ultrasound[15–17] to measure the optical distortions of biological tissue.

The wavefront correction strategy in transmission (i.e., with two optical accesses) was successfully adapted in our former work to stabilize two laser beams of a laser Doppler velocimeter (LDV) through a fluctuating water–air phase boundary.[18] However, the acquisition of the distortion in transmission is not always possible. For instance, a high-pressure cleaner generates a jet of water, which has a radially open phase boundary that inhibits an undisturbed optical access from any direction. It is very difficult to generate a guide star inside the jet without significantly disturbing the flow. To overcome this, we developed the Fresnel guide star (FGS) technique.[19,20] The strategy is to illuminate the surface with a laser source where the wavefront shape is known and to measure the wavefront of the reflected beam, i.e., the Fresnel reflex. With both information, an observer is able to determine the shape of the surface similar to deflectometry[21,22] and to calculate the deflection of the light propagating through the surface. This opens up the possibility to correct for wavefront distortions stemming from a single interface with a single optical access. However, the FGS requires reference and/or calibration measurements. Up to now, the approaches for calibration and the presented results[19] have a proof of principle character. In this paper, we present tailoring of the FGS technique for realistic flow measurement inside of a liquid jet.

2 Setup

2.1 *Velocity Measurement Technique*

A LDV is based on a Mach–Zehnder interferometer. A laser beam is split up and both partial beams are crossed at the measurement volume. At this intersection, both beams interfere and create nearly parallel fringes perpendicular to the crossing angle. The distance d between the light sheets is a function of the crossing half angle θ, the laser wavelength λ, the longitudinal coordinate z, and the position of the beam waist z_w with respect to the position of the beam intersection and can be calculated by Eq. (1).[23] The Rayleigh length z_R is defined by $z_R = \pi w_0^2/\lambda$, where w_0 is the radius of the beam

*Address all correspondence to: Hannes Radner, E-mail: hannes.radner@tu-dresden.de

waist. Equation (1) can be approximated to Eq. (2) if w_0 or z_w are large

$$d = \frac{\lambda}{2\ \sin(\theta)}\left[1 + \frac{z\cos^2\theta(z\cos^2\theta - z_w)}{z_R^2\cos^2\theta - z_w(z\cos^2\theta - z_w)}\right], \tag{1}$$

$$d \approx \frac{\lambda}{2\ \sin(\theta)}. \tag{2}$$

If a particle crosses the fringe system, it periodically scatters light, which is sampled by a photodetector. The velocity v perpendicular to the fringe system can then be calculated by the product of the fringe spacing d and the Doppler frequency f, respectively

$$v = d \cdot f. \tag{3}$$

For a reliable Doppler peak detection, a high interferometric contrast of the fringe system is desired and for a low standard deviation, the calibrated fringe spacing d should be kept constant.

2.1.1 *Influence of distortions on the measurement*

Former investigations[18] showed that a laser Doppler flow measurement is mainly influenced by tip and tilt deflections of surface waves. This can be explained by the small diameter of the laser spot compared with the wavelength λ_w of the surface waves. For the liquid jet setup, see Sec. 2.2, the laser spot size at the interface is about 56 μm and the surface wavelength is about 17.7 mm.

The surface wavelength is calculated by Eq. (4), where c is the mean flow velocity and f_w is the maximum frequency of the surface fluctuation, see Sec. 2.3

$$\lambda_w = \frac{c}{f_w} = \frac{1.436\ \text{m}}{81\ \text{Hz s}} \approx 17.7\ \text{mm}. \tag{4}$$

As this assumption holds for most applications, in the following just tip/tilt deflections will be considered as the error source. The deflections at the phase boundary have two effects on the LDV. If the crossing angle θ between both partial beams changes, the fringe spacing varies and thus leads to an increased uncertainty for the velocity. If the beams are deflected perpendicularly to the plane spanned by the two partial beams, the interference contrast is decreased or in the worst case both beams miss each other, no fringe pattern is generated and so the measurement fails.

The influence of the fluctuating surface on the burst signals can be neglected, hence they have a frequency of about 1 MHz and the surface is quasistatic with a maximum fluctuation frequency of 81 Hz for them.

2.2 *Optical Setup*

The setup for the velocity measurement inside of a liquid jet using the FGS technique is shown in Fig. 1. The light source is a 532-nm Nd:YAG laser. A beam splitter is used to create the two required beams with a diameter of about 1.5 mm. Each partial beam is collimated and the beam waist is positioned in the measurement volume by L1a/b with a focal length F of 60 mm and a diameter D of 30 mm, respectively. After that, each beam is imaged by a Keplerian telescope (L2a/b $F = 100$ mm, $D = 35$ mm and L3a/b $F = 150$ mm, $D = 35$ mm) from a biaxial voice coil-driven mirror (OIM101, optics in motion, ±3-deg optical deflection, 3-dB bandwidth for small angles 550 Hz, 60 Hz for full range) onto the jet surface to adjust the incident beam angle. The scattered light from the measurement volume is captured by L6 ($F = 75$ mm and $D = 50.8$ mm) and focused on a fiber-coupled photodetector to measure the Doppler frequency (the fiber has a core diameter of

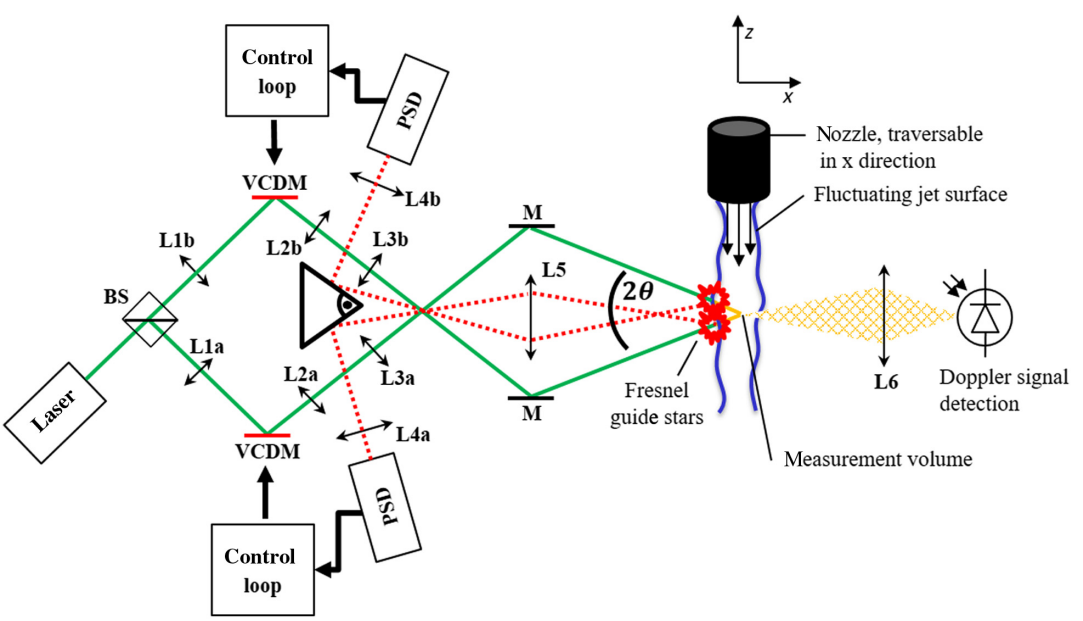

Fig. 1 Optical setup of the adaptive LDV. For details on the deflection of the surface, see Fig. 4. BS, beam splitter; VCDM, voice coil driven mirror; PSD, position-sensitive device; L, lenses. The jet diameter was about 10 mm and the flow speed was about 1.44 m/s.

400 μm and a numerical aperture of 0.39). The spacing of the fringe system was adjusted to ~2.1 μm in the jet and the full width at half maximum of the beam diameter was set to 30 μm resulting in a measurement volume of ~30 μm × 320 μm. As the Fresnel reflexes are very close to each other on the jet surface, the reflected beam angles cannot be directly measured with two-dimensional (2-D) PSDs because at high distortions they would illuminate the same detector. This is solved by imaging the surface with L5 ($F = 75$ mm, $D = 50.8$ mm) onto a knife-edge right-angle prism mirror (MARK25-P01, Thorlabs) from where the lenses L4a/b ($F = 80$ mm, $D = 30$ mm) focus the reflexes on the position sensitive devices (PDP90A, Thorlabs, 3-dB bandwidth 15 kHz, sensor size 9 mm × 9 mm). To maximize the number of calculation cycles per second, each beam has its own control loop. As a liquid, a mixture of 83% glycerin and 17% water is used to reduce the fluctuation frequency of the jet surface.

The diameter of the jet is about 10 mm and the flow velocity is about 1.436 m/s. A seeding consisting of silver-coated hollow glass spheres with a diameter of 10 μm was added to the fluid. The optical laser power in the measurement volume was 12 mW.

The LDV of this setup offers no direction sensitivity, but since the jet has a main flow direction this is not required. However, if the application would require direction sensitivity an acoustic optical modulator could be integrated in one of the partial beams behind the beam splitter to create a heterodyne interferometer.[24]

2.3 *Characterization of the Distortion and Influence on the Velocity Measurement*

The fluctuation of the jet surface was characterized by evaluating one of the reflected beams with the corresponding PSD sensor (see Fig. 1). For the wavefront correction system, two values are of main interest. First, the maximum surface fluctuation frequency, which determines how fast the control loop needs to be. Second, the maximum occurring amplitude to ensure that the actuator has enough range. In the flow direction, the maximum fluctuation frequency was determined to be about 81 Hz by fitting two lines to the amplitude spectrum with a linear least square fit on the right- and left side of the cutoff frequency (see Fig. 2). The green line represents the noise level of the PSD, and the red line represents the spectrum of the distortion. The density function for different tilt angles (in flow direction) was measured with 10,000 samples over 5 sec and is shown in Fig. 3. The maximum angle was found to be about 0.25 deg. Perpendicular to the flow direction the figures are qualitatively similar. The maximum frequency was about 67 Hz, and the maximum angle was about 0.05 deg.

2.4 *Fresnel Guide Star Technique*

The FGS technique uses the reflection at a distortion, e.g., a phase boundary, to gain all required information to correct the influence of the distortion. Most importantly, this is achieved with a single optical access. Therefore, the transmitted beam angle α_{2i} inside the jet is not measured directly; an observer is used to estimate it. It calculates the transmitted beam path from the measured Fresnel reflex of the FGS using the law of reflection and Snell's law. At the jet surface, the three-dimensional (3-D) relationship can be simplified

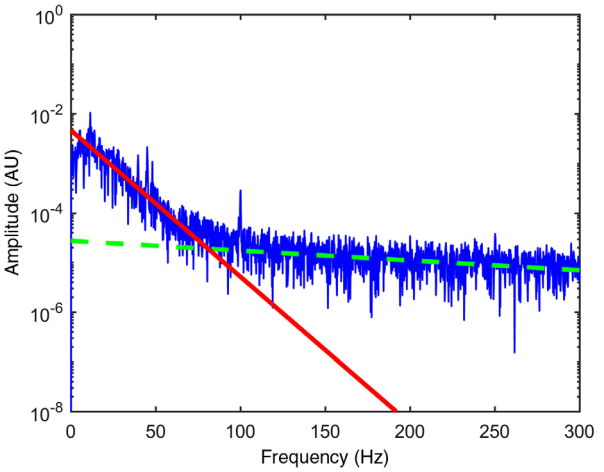

Fig. 2 Measured amplitude spectrum of the deflection of the jet surface in the flow direction (interface between liquid and air). Two lines were fitted to the data with a linear least square fit to determine the cutoff frequency of 81 Hz. The green line represents the noise level of the PSD and the red line represents the spectrum of the distortion.

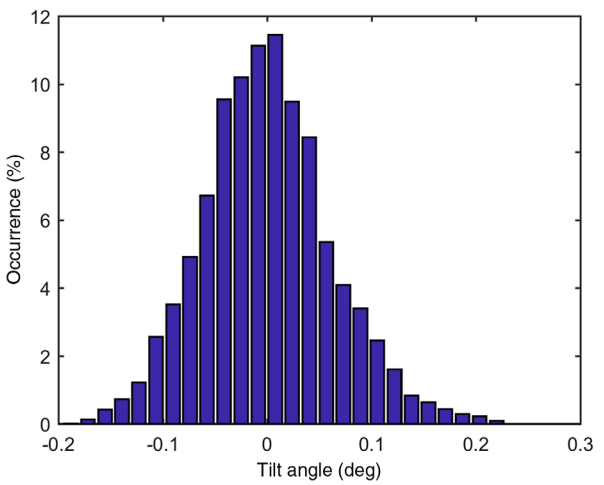

Fig. 3 The measured histogram shows the density function of different tilt angles (in flow direction) of the jet surface. The standard deviation is 0.0619 deg.

into a 2-D relationship for the local x- and y-directions, where $i = \{x, y\}$, as shown in Fig. 4. If the incident angle α_{1i} and the reflected angle β_{1i} are measured and surface height changes are neglected, it is possible to determine the local tilt angle γ_i of the surface normal using the equation

$$\gamma_i = \frac{\beta_{1i} - \alpha_{1i}}{2}. \tag{5}$$

If the tilt angle γ_i of the surface is known, the deflection of the transmitted light ray T can be calculated using the Snell's law. With the estimated transmitted angle, the incident angle can be adjusted as needed to achieve the desired beam path behind the surface.

However, although it is the strength of the FGS technique that just a single optical access is required to measure all required information for correction, the usage of the reflection at the phase boundary is accompanied by a drawback: the light from the measurement volume propagates through

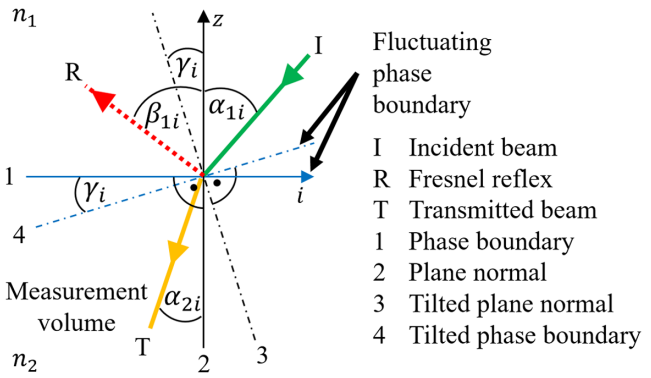

Fig. 4 Two-dimensional scheme of the laser beam deflection *I* (incidence), *T* (transmission), and *R* (reflection) at the interface of two media with refractive indexes $n_1 < n_2$. The FGS is generated at the phase boundary by the Fresnel reflex.

the phase boundary (refractive index transition from n_2 to n_1), whereas the FGS just propagates in one medium (with refractive index n_1, compare Fig. 4). Both refractive indices have to be known to apply Snell's law for the calculation.

Furthermore, knowledge of the exact position of all involved laser beams relative to the surface is required. As this is not possible due to uncertainties of the position and orientation of all components, an approach based on eigencalibration was developed.[19] During this process, two properties are calibrated. First, the axes of the light modulator manipulating the incident angles α_{1i} have to be aligned with the reflected angle β_{1i} axes on the detectors (PSDs). This is important to simplify the 3-D problem, which would lead to a complex multiple-input multiple-output control loop, into two equal standard control loops with a single-input and single-output.

To achieve this, a decoupling matrix M can be used. It performs a coordinate transform, where $\Delta\alpha$ represents the incident angle deviation and $\Delta\beta$ is the deviation of the reflected beam angle. The multiplication $M \cdot \Delta\alpha$ now gives information how the incident x- and y-axes are oriented to the reflected x- and y-axes

$$M \cdot \Delta\alpha = \Delta\beta, \tag{6}$$

$$\begin{pmatrix} M_{\alpha_x\beta_x} & M_{\alpha_y\beta_x} \\ M_{\alpha_x\beta_y} & M_{\alpha_y\beta_y} \end{pmatrix} \cdot \begin{pmatrix} \Delta\alpha_x \\ \Delta\alpha_y \end{pmatrix} = \begin{pmatrix} \Delta\beta_x \\ \Delta\beta_y \end{pmatrix}. \tag{7}$$

To determine the decoupling matrix, a static surface is needed. The light modulator deflects the light by $\Delta\alpha_x$ in the x-axis and $\Delta\alpha_y$ is kept zero. The displacement $\Delta\beta_x$ and $\Delta\beta_y$ on the detector is measured, and the first column of M can be filled. The same strategy is used to fill the second column. The multiplication $M^{-1} \cdot \Delta\beta$ performs a coordinate transformation of the measured deflection on the detector and decouples the control loops of both axes.

Second, a calibration for the relation between α_{1i}, α_{2i}, and β_{1i} is needed because the precise refractive index is unknown and due to uncertainties of the position and orientation of the components in the setup, the precise angles with respect to the surface normal are difficult to determine.

A simultaneous direct measurement of the incident, reflected, and transmitted beam angles generating a lookup table circumvents the need to use Snell's law to calculate the beam path. In our former work,[19] two laser beams were stabilized through a fluctuating surface of a basin filled with water. Here both calibration steps were easily be realized, as the surface was not fluctuating and the transmitted beams were observable while the calibration was in progress.

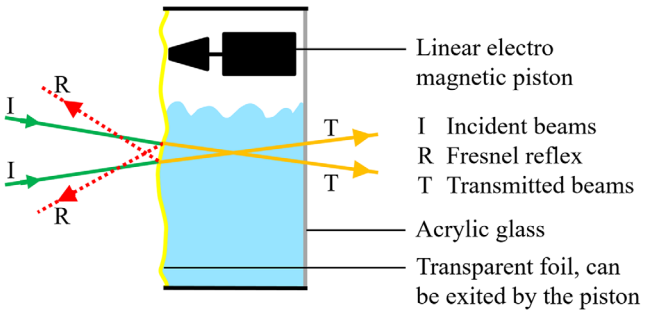

Fig. 5 The calibration target replaces the jet in Fig. 1 for calibration purposes with additional PSDs to observe the deflection of the transmitted beams. An electromagnetic piston can excite the foil.

For a measurement inside of a liquid jet, this calibration steps are a challenge as it is not possible to calibrate directly at a fluctuating surface and to measure the transmitted beam deviation. To overcome this, a special calibration target (see Fig. 5) was designed to calibrate the observer and the decoupling matrix. It is a hollow cuboid, where the front is replaced by a thin transparent foil and the back by acrylic glass. The foil generates similar Fresnel reflex as the jet surface and it can be deflected by an electromagnetic piston. The target is filled with the same fluid as used for the jet. For the calibration process, the jet is replaced with the target. The decoupling matrix can now be calibrated at a nonmoving surface. With this target, it is also possible to calibrate the observer by simultaneously measuring the incident, reflected, and transmitted beam angles. Therefore, the electromagnetic piston periodically excites the surface, a lookup table of the refractive relationship is generated and a plane can be fitted to the data. The active control loop then tries to stay at the same isocline of the plane by steering the incident angle to keep the transmitted beam stable.

A limitation of the FGS technique is that only smooth fluctuating interfaces can be corrected (no breaking liquid jets with ligaments or with droplets) and surface height changes have to be tolerable because they can lead to an error of the beam estimation with the lookup table. It should also be noted that the fitted plane used by the observer represents a linear approximation $[\sin(x) \approx x]$ of Snell's law and is only valid for small deflection angles. If this approximation is insufficient, a higher order polynomial fit or a fit with trigonometric functions could be used. For the presented setup, the angles are very small and a linear fit was found to be well sufficient.

2.5 *Control Loop*

The schematic control loop is shown in Fig. 6. It is realized on a digital signal processor (DSP, dsPIC33EP512GP502, Microchip). The DSP samples the 2-D PSD to measure the 2-D deflection angle of the Fresnel reflex. To align the 2-D PSD axis with the axes of the adaptive mirror, the raw data are fed into the decoupling matrix. The decoupled data are used by the observer to estimate the

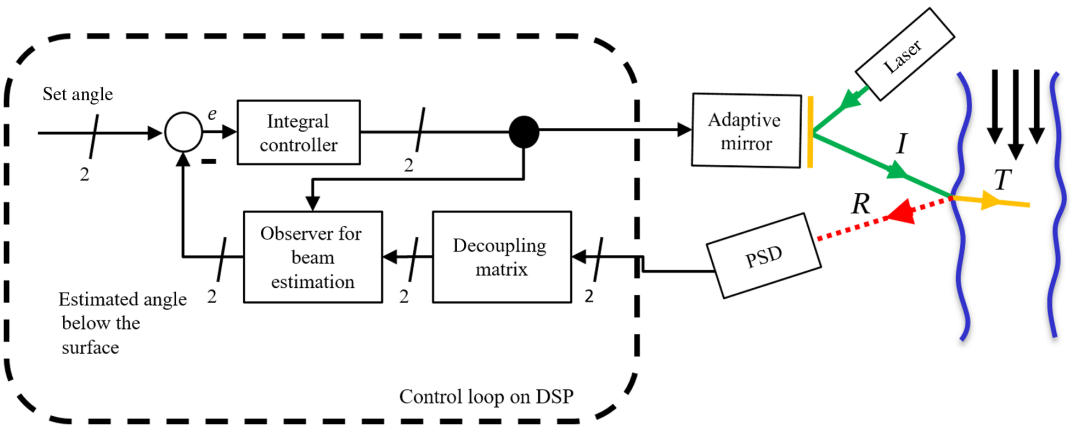

Fig. 6 Setup of the control loop for only one beam path. It samples the reflected angle in the *x*- and *y*-directions with a PSD. A decoupling matrix performs a coordinate transform, so that the incident angle in the *x*-direction matches the detected *x*-direction. The same applies for the *y*-direction. The measurement data are fed into an observer, which estimates the transmitted beam path. This result is compared with the set value and the deviation is fed into an integral controller, which steers the adaptive mirror.

transmitted beam angle from the incident and reflected beam angles. The estimated angle is compared with a set value and the deviation is passed to an integral controller, which steers the adaptive mirror as a light modulator.

The DSP reaches about 10,000 calculation cycles per second. The maximum frequency up to which the control loop is able to suppress distortions was determined by measuring the transfer function $H(f)$ of the open control loop without the integral controller. A phase of -90 deg is reached at 160 Hz (see Fig. 7). With an integral controller and a theoretical phase margin of zero, distortions up to 160 Hz could be suppressed. The performance is mainly limited by the steering mirrors, whose 3-dB frequency for full amplitude is about 60 Hz. For small amplitudes, the 3-dB frequency can reach 550 Hz because of nonlinearities of the voice coil actuation. However, 160 Hz is well sufficient to suppress the occurring distortions of up to 81 Hz, see Fig. 2.

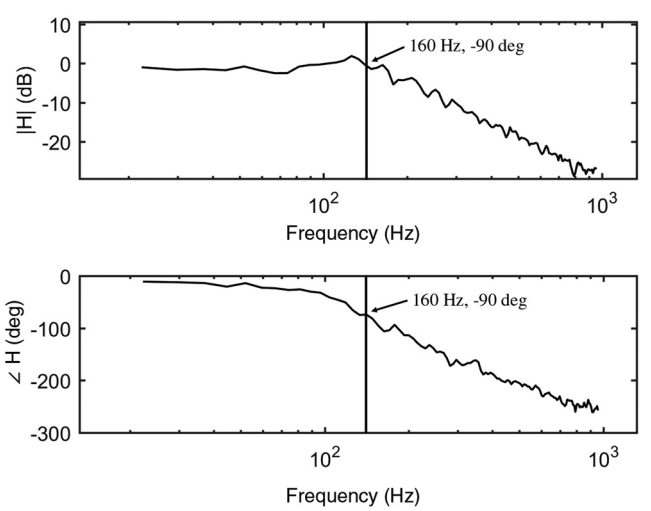

Fig. 7 Measured Bode diagram of the transfer function $H(f)$ of the open loop without integral controller. A phase shift of -90 deg is reached at 160 Hz, which allows an integral controller to suppress distortions and aberrations up to this frequency.

3 Measurement Inside of the Liquid Jet

The system was tested with a traversed flow measurement inside the liquid jet (see Fig. 8). The measurement volume was placed at the center and was traversed in the *x*-direction by 250 μm in steps of 50 μm. The traversing range is mainly limited by the numerical aperture of the detection optics, because it cannot capture the reflected beams anymore. The standard deviation was about 0.02 m/s or 1.5%. To characterize the wavefront correction performance, the mean validation rate was used. A burst signal is valid if the interference contrast exceeds 22%. The value is chosen heuristically. It should be as low as possible to evaluate as many burst signals as possible, but it must be high enough to ensure proper Doppler peak detection in the Fourier spectrum of the burst signal. The mean SNR of the burst signals was about 12 dB. The active control loop reached about 15% more valid burst signals as without stabilization. Thereby, the measurement volume could be traversed by 250 μm in the *x*-direction (as shown in Fig. 1) without a drop of the validation

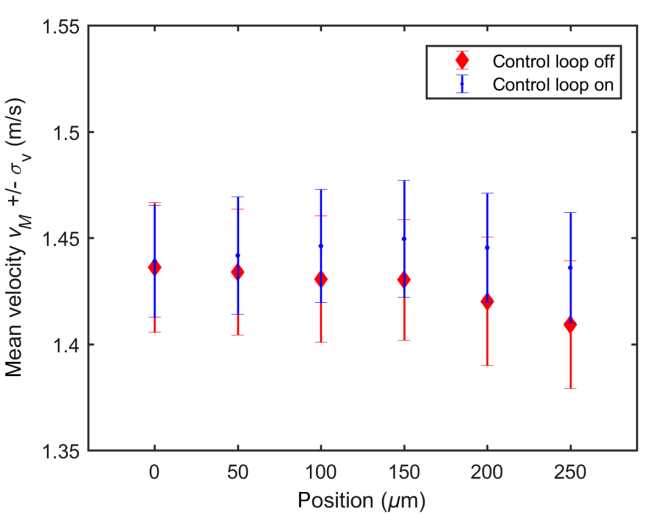

Fig. 8 Measured velocity profile inside the liquid jet, traversed in the *x*-direction (compare with Fig. 1). The error bars represent the standard deviation of the mean velocity value.

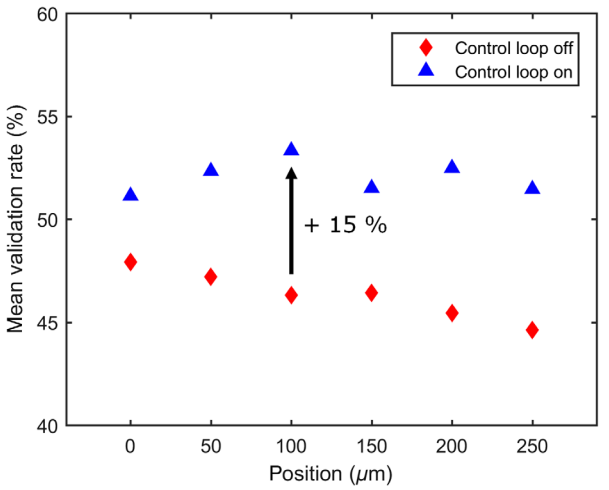

Fig. 9 Measured validation rate as a function of the *x*-position (compare to Fig. 1). The validation rate is defined as the ratio between the number of valid burst signals and the total signal number.

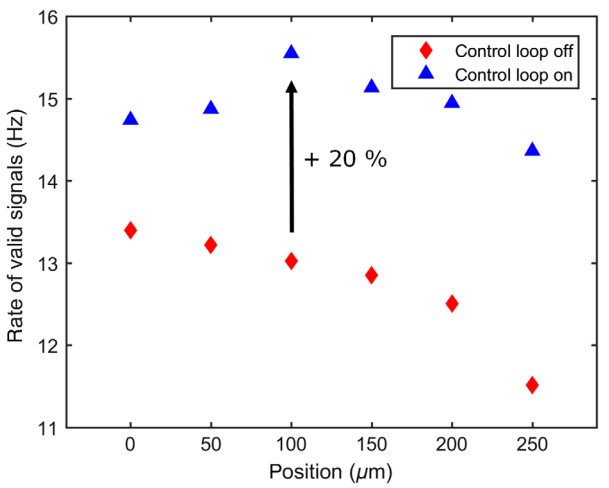

Fig. 10 Measured rate of valid signals in Hz for constant seeding density, traversed in the *x*-direction (compare with Fig. 1).

rate (see Fig. 9). A validation rate of 100% was not reached. Possible reasons are observer uncertainties, caused by neglected height changes of the surface. Furthermore, the transfer function of the steering mirrors is nonlinear and highly depends on the amplitude, which degrades the performance of the control loop. The increased validation rate enables a 20% higher burst rate per second at the same seeding density as shown in Fig. 10.

4 Conclusion

To measure velocity profiles inside a liquid jet through the fluctuating interface, we presented an adaptive optical measurement system, which stabilizes both laser beams of an LDV inside the jet. It estimates the beam path behind the surface by evaluating the incident beam angle and reflected beam angle of the Fresnel reflex with an observer. With this approach, only one optical access through the phase boundary is needed for the measurement. To demonstrate the performance of the wavefront correction technique, the flow profile inside of a liquid jet was measured with a constant increased rate of valid signals.

The FGS technique has been proven to correct optical distortions caused from fluctuating interfaces and can improve any optical measurement technique where optical distortions degrade the measurement. It can improve many well-established metrology systems e.g., particle imaging velocimetry to expand the area of applications. This could be the measurement of film flows on an opaque substrate in cooling applications,[25] where the fluctuating surface degrades the measurement.

Disclosures

The authors declare no conflict of interests.

Acknowledgments

The authors thank the Deutsche Forschungsgemeinschaft (DFG) for funding and supporting this work within a Reinhart Koselleck project (CZ 55/30).

References

1. X. Wang et al., "Modeling and performance limits of a large aperture high-resolution wavefront control system based on a liquid crystal spatial light modulator," *Opt. Eng.* **46**(4), 044001 (2007).
2. S. Abado, S. V. Gordeyev, and E. J. Jumper, "Adaptive-optic system requirements to mitigate aero-optical aberrations as a function of viewing angle," *Opt. Eng.* **53**(10), 103103 (2014).
3. J. Chen et al., "Experimental evaluation of a positive-voltage-driven unimorph deformable mirror for astronomical applications," *Opt. Eng.* **54**(11), 117103 (2015).
4. A. V. Goncharov et al., "Adaptive optics schemes for future extremely large telescopes," *Opt. Eng.* **41**(5), 1065–1072 (2002).
5. P. Jiang et al., "Comparison of the Shack–Hartmann and plenoptic sensor in closed-loop adaptive optics system," *Opt. Eng.* **55**(3), 033105 (2016).
6. M. Laslandes et al., "Mirror actively deformed and regulated for applications in space: design and performance," *Opt. Eng.* **52**(9), 091803 (2013).
7. B. K. McComas and E. J. Friedman, "Wavefront sensing for deformable space-based optics exploiting natural and synthetic guide stars," *Opt. Eng.* **41**(8), 2039–2049 (2002).
8. D. Ren and B. Dong, "Demonstration of portable solar adaptive optics system," *Opt. Eng.* **51**(10), 101705 (2012).
9. E. Vernet-Viard et al., "Layer-oriented wavefront sensor for a multiconjugate adaptive optics demonstrator," *Opt. Eng.* **44**(9), 096601 (2005).
10. R. Q. Fugate et al., "Measurement of atmospheric wavefront distortion using scattered light from a laser guide-star," *Nature* **353**, 144–146 (1991).
11. E. H. Zhou et al., "Focusing on moving targets through scattering samples," *Optica* **1**(4), 227 (2014).
12. O. Katz et al., "Noninvasive nonlinear imaging through strongly-scattering turbid layers," *Optica* **1**(3), 170–174 (2014).
13. J. Bertolotti et al., "Non-invasive imaging through opaque scattering layers," *Nature* **491**, 232–234 (2012).
14. C.-L. Hsieh et al., "Imaging through turbid layers by scanning the phase conjugated second harmonic radiation from a nanoparticle," *Opt. Express* **18**(20), 20723–20731 (2010).
15. B. Judkewitz et al., "Speckle-scale focusing in the diffusive regime with time reversal of variance-encoded light (TROVE)," *Nat. Photonics* **7**, 300–305 (2013).
16. G. Lerosey and M. Fink, "Merging the best of two worlds," *Nat. Photonics* **7**(4), 265–267 (2013).
17. X. Xu, H. Liu, and L. V. Wang, "Time-reversed ultrasonically encoded optical focusing into scattering media," *Nat. Photonics* **5**, 154–157 (2011).
18. L. Büttner, C. Leithold, and J. Czarske, "Interferometric velocity measurements through a fluctuating gas-liquid interface employing adaptive optics," *Opt. Express* **21**(25), 30653–30663 (2013).
19. H. Radner, L. Büttner, and J. Czarske, "Interferometric velocity measurements through a fluctuating phase boundary using two Fresnel guide stars," *Opt. Lett.* **40**(16), 3766–3799 (2015).
20. N. Koukourakis et al., "Wavefront shaping for imaging-based flow velocity measurements through distortions using a Fresnel guide star," *Opt. Express* **24**(19), 22074–22087 (2016).
21. G. Häusler et al., "Microdeflectometry—a novel tool to acquire three-dimensional microtopography with nanometer height resolution," *Opt. Lett.* **33**(4), 396–398 (2008).

22. L. Huang, C. S. Ng, and A. K. Asundi, "Dynamic three-dimensional sensing for specular surface with monoscopic fringe reflectometry," *Opt. Express* **19**(13), 12809–12814 (2011).
23. P. C. Miles, "Geometry of the fringe field formed in the intersection of two Gaussian beams," *Appl. Opt.* **35**(30), 5887–5895 (1996).
24. H. E. Albrecht et al., *Laser Doppler and Phase Doppler Measurement Techniques*, Springer Science & Business Media (2013)
25. W. Ambrosini, N. Forgione, and F. Oriolo, "Statistical characteristics of a water film falling down a flat plate at different inclinations and temperatures," *Int. J. Multiphase Flow* **28**(9), 1521–1540 (2002).

Hannes Radner received his diploma degree in electrical engineering from the Technische Universität Dresden, Germany, in 2014. Since 2014, he is a member of the academic staff of the laboratory for measurement and sensor system techniques at the Technische Universität Dresden. His research interests include laser metrology in combination with wavefront correction systems, the system design, and implementation of FPGA-based control loops for adaptive optics. He has a SPIE student membership.

Lars Büttner studied physics at Clausthal University of Technology, Germany. Since 1999, he was a research fellow with the Laser Zentrum Hannover, Germany. He received his PhD in physics from Leibniz Universität Hannover, in 2004. Since 2005, he is the head of the Flow Measurement Group at the Laboratory for Measurement and Sensor System Techniques at Technische Universität Dresden, Germany. His current research interests include laser- and ultrasound-based measurement techniques and adaptive optical systems.

Jürgen Czarske holds a PhD in electrical engineering from Leibniz University of Hannover. In September 2014, he was appointed as a chair professor of Measurement and Sensor System Techniques at TU Dresden. He is a fellow of the SPIE, EOS, and OSA. He has published over 150 international papers in peer-reviewed journals and holds over 15 patents. His main research field is system engineering with ultrasound and laser waves.